Underexpression of RhoH in Hairy Cell Leukemia

Sylvie Galiègue-Zouitina,[1] Laure Delestré,[1] Caroline Dupont,[1] Xavier Troussard,[2] and Carl Simon Shelley[1,3,4]

[1]Institut National de la Santé et de la Recherche Medicale U.837, Centre Jean-Pierre Aubert, Institut de Recherches sur le Cancer de Lille and Université Droit et Santé de Lille II, Lille, France; [2]Laboratoire d'Hématologie, Centre Hospitalier Universitaire de Caen, Caen, France; [3]Renal Unit, Massachusetts General Hospital, Harvard Medical School, Boston, Massachusetts; and [4]Gundersen Lutheran Medical Foundation, La Crosse, Wisconsin

Abstract

The cause of hairy cell leukemia (HCL) is unknown. Current treatments seem effective only for a limited period of time. In addition, a significant proportion of patients remain refractive to all treatment options. These considerations indicate the need to develop alternative therapeutic strategies for HCL. Here, we report that HCL is characterized by underexpression of RhoH. *In vitro* reconstitution of RhoH expression inhibits the aberrant adhesion and transendothelial migration that drives disease pathogenesis. In an *in vivo* model of HCL, RhoH reconstitution limits malignant progression and protects against mortality. These findings provide the proof of principle that RhoH reconstitution represents a potential new approach to the treatment of HCL. [Cancer Res 2008;68(12):4531–40]

Introduction

Hairy cell leukemia (HCL) is a chronic lymphoproliferative disease, the cause of which is unknown (1–3). The disease is characterized by pancytopenia, hepatomegaly, splenomegaly, leukocytosis, and neoplastic mononuclear cells in the peripheral blood, bone marrow, liver, and spleen (1–3). Purine analogues are the current treatments of choice (2, 4, 5). However, a significant proportion of HCL patients remain refractive to these compounds (4, 5). In addition, disturbing new evidence that shows purine analogous only delay disease progression rather than provide a cure has emerged (6). HCL is a disease of late middle age (2, 3). Consequently, in countries with aging populations, HCL is set to become an increasing health care burden. These considerations highlight the need to develop alternative approaches to the treatment of HCL.

The malignant cells of HCL are diagnosed biochemically by aberrant expression of tartrate resistant acid phosphatase and the β2-integrin CD11c (7–12). Critical to the expression of the *CD11c* gene is its interaction with the transcription factor activator protein-1 (AP-1) (13). Normally, AP-1 expression is transient and mediates induction of *CD11c* in response to specific differentiation signals (14). However, in the neoplastic lymphocytes of HCL, AP-1 is expressed constitutively, thus driving abnormal concomitant expression of *CD11c* (13). One of the most important mechanisms controlling AP-1 expression is protein phosphorylation regulated by the Ras family of proto-oncogenes (15–25). In previous studies, we determined that, in HCL, Ras activation drives chronic expression of AP-1 that in turn drives the abnormal expression of *CD11c* diagnostic of the disease. Here, we report that, in addition to abnormal overexpression of AP-1 and Ras, HCL is also characterized by abnormal underexpression of RhoH (26, 27). This molecule is expressed exclusively by hematopoietic cells and lacks GTPase activity. Due to its inability to hydrolyze GTP, RhoH remains GTP bound and so acts as a noncompetitive inhibitor of members of the Ras family that cycle between forms bound by GTP and GDP (28, 29). Reconstitution of RhoH expression reduces HCL proliferation and both homotypic and heterotypic adhesion *in vitro*. RhoH reconstitution also reduced the process of transendothelial migration that is central to HCL pathogenesis. Finally, in an *in vivo* xenograft mouse model of HCL, we found that RhoH reconstitution inhibited malignant progression and protected against mortality. These findings thus provide proof-of-principle that RhoH reconstitution represents a promising new therapeutic strategy to combat HCL.

Materials and Methods

Cell culture. The hairy cell line Mo, the T-cell lines CEM and HSB-2, and the B-cell lines Raji, Namalwa, Daudi, and U-266 were obtained from the American Type Culture Collection and grown according to their specifications (30–35). The B-cell line VAL was provided by Dr. Christian Bastard (Laboratoire de Génétique Oncologique, Centre Henri Becquerel; ref. 36). The Karpas 231 B-cell line was provided by Dr. Abraham Karpas (University of Cambridge; ref. 37). The hairy cell line HC-1 was obtained from the Deutsche Sammlung von Mikroorganismen und Zellkulturen GmbH and grown according to their specifications (38). The hairy cell line EH was provided by Dr. Guy B. Faguet (Veterans Administration Medical Center; ref. 39). The hairy cell line ESKOL was provided by Edward F. Srour (Indiana University School of Medicine; ref. 40). The hairy cell lines JOK-1, Hair-M, and JC-1 were provided by Jorn Koch (Aarhus University Hospital; ref. 41). Human microvascular endothelial cells (HMEC-1) were a gift of Dr. Sean P. Colgan (Brigham and Women's Hospital; ref. 42). $CdCl_2$ was obtained from Fluka Chemie AG and used at concentrations of 1 or 10 μmol/L, where indicated. Lipopolysaccharide (LPS) was obtained from EMD Biosciences, Inc., and used at a final concentration of 100ng/mL, where indicated.

Isolation of B-lymphocytes from human peripheral blood and spleens. After informed consent, peripheral blood was drawn from normal volunteers and patients with HCL. Also, after informed consent, spleens were removed from patients with chronic immune idiopathic thrombocytopenia (ITP) or splenic lymphoma with villous lymphocytes (SLVL). Subsequent morphologic examination indicated that the spleens of ITP patients were normal. Blood and spleen leukocytes were prepared by Ficoll gradient centrifugation and frozen in liquid nitrogen. After thawing, cells were washed twice in RPMI 1640 containing 15% fetal bovine serum (FBS) and then resuspended in ice-cold PBS supplemented with 0.5% FBS and 2 mmol/L EDTA. B-lymphocytes were isolated by negative selection using the B Cell Isolation Kit II (Miltenyi Biotec). Cells isolated from HCL patients were determined to be over 90% positive for surface expression of CD19 and CD103 by flow cytometry. Cells isolated from normal individuals were over

Requests for reprints: Carl Simon Shelley, Gundersen Lutheran Medical Foundation, La Crosse Medical Health Science Center, 1300 Badger Street, La Crosse, WI 54601. Phone: 608-789-8952; Fax: 608-775-6602; E-mail: carlsimonshelley@yahoo.com.

©2008 American Association for Cancer Research.

doi:10.1158/0008-5472.CAN-07-5661

Downloaded from cancerres.aacrjournals.org on January 5, 2016. © 2008 American Association for Cancer Research.

90% positive for CD19, but negative for CD103. Cells isolated from patients with SLVL or ITP were over 90% positive for CD19. Before RNA isolation, B-lymphocytes were washed once in PBS supplemented with 0.5% FBS but lacking EDTA.

Plasmid construction. The activity of the *CD11c* promoter was assessed using the expression vector pATLuc that contains a promoterless firefly *luciferase* reporter gene (43). PCR was used to generate a fragment of the *CD11c* gene representing nucleotides −128 to +36 relative to the major transcription initiation site. This fragment was then subcloned into the "filled-in" *Hin*dIII site of pATLuc to generate p11c-Wt (13, 44). The ability of RhoH to repress the *CD11c* promoter was assessed using the expression constructs pCMV-RhoH and pMEP-RhoH. These were generated by first isolating the *Eco*RI/*Xba*I and *Kpn*I/*Xba*I fragments of pcDNA3-VSVG-RhoH-Wt that encode RhoH tagged at its NH_2 terminus with the vesicular stomatitis virus glycoprotein (VSVG) epitope. The isolated *Eco*RI/*Xba*I fragment was then cloned between the *Eco*RI and *Xba*I sites of pcDNA3.1Zeo(+) (pCMV; Invitrogen Corp.) to produce pCMV-RhoH. The *Kpn*I/*Xba*I fragment containing *RhoH* was cloned between the *Kpn*I and *Nhe*I sites of pMEP4 (Invitrogen Corp.) to generate pMEP-RhoH. The activity of the *RhoH* gene promoter was assessed using the expression vector pGL4.14[*Luc2/Hygro*] that contains a promoterless firefly *luciferase* reporter gene (Promega Corp.). PCR was used to generate a fragment of the *RhoH* gene representing nucleotides −236 to +67 relative to a transcription initiation site used in B-lymphocytes. This fragment was then subcloned into the *Hin*dIII site of pGL4.14[*Luc2/Hygro*] to generate pGL4-RhoH. The transfection control plasmid pSV-βGal that directs expression of β-galactosidase was purchased from Promega Corp.

RNA isolation. Total RNA was isolated from cell lines and human B-lymphocytes by use of the High Pure RNA Isolation kit (Roche Diagnostics). The procedure included a DNase-I treatment to eliminate genomic DNA contamination. Amounts and quality of RNA were evaluated by UV spectroscopy using an Agilent 2100 Bioanalyser (Agilent Technologies).

PCRs. The cDNA templates for quantitative reverse transcriptase–PCR (Q-RT-PCR) were prepared by random priming of 5 μg of total RNA with 200 units of Moloney murine leukemia virus reverse transcriptase in a final volume of 100 μL. The quality and quantity of templates were evaluated by analysis of ABL mRNA in accordance with the recommendations of Europe Against Cancer (45). The B-cell line Namalwa that expresses high levels of ABL and RhoH mRNA was used to produce calibration curves that evaluated PCR efficiency. RhoH and ABL mRNA were measured separately using TaqMan technology (Applied Biosystems). Real-time quantitative PCR primer pairs and probes were chosen with the assistance of the computer program Primer Express (Applied Biosystems). Due to heterogeneity at the 5′ end of RhoH mRNA, care was taken to design PCR primers that amplified all RhoH transcripts (46). The sense primer used had the nucleotide sequence 5′-TTTGGAAACTTCTCCTTCACACAC-3′, and the antisense primer had the sequence 5′-GCCCATCCAAGCACCGT-3′. The size of the PCR product resulting from the use of these primers was 81 bp and, therefore, compatible with good amplification efficiency. The RhoH probe had the sequence 5′-AGTTGAAGACTAGGCTTT-3′ and was labeled at its 5′-end with 6-carboxy-fluorescein phosphoramidite (FAM) and at its 3′-end with a nonfluorescent quencher. The ABL probe that was used as a control for cDNA quantity and quality was also labeled with FAM at its 5′-end but with 6-carboxy-tetramethyl-rhodamine as a quencher at its 3′-end. Each PCR reaction was performed in a 25-μL total volume, using 12.5 μL of 2 × UDG Master Mix (Applied Biosystems), 10 μmol/L each of sense and antisense primer, and ∼100 ng of cDNA template. Each PCR run included samples containing no cDNA and Namalwa cDNA that produced calibration curves for *ABL* and *RhoH* gene expression. The relative level of endogenous RhoH expression was calculated by dividing the quantitative level of RhoH expression by the quantitative level of ABL expression. All relative levels of RhoH expression were determined from two independent preparations of RNA, each of which was used in two independent cDNA synthesis reactions. Each cDNA synthesis was then analyzed by two independent quantitations performed in duplicate. Expression of recombinant RhoH tagged with the VSVG epitope was evaluated by RT-PCR using a sense primer with the nucleotide sequence 5′-ATGGGTTACACCGACATCGAGATGACC-3′ and an antisense primer with the nucleotide sequence 5′-TCTCGTACACTGTGGGCTTGTAGGC-3′. This primer pair generates PCR products only from transcripts that encode VSVG-RhoH and not from transcripts that originate from the endogenous *RhoH* gene. Evaluation of RhoH expression by RT-PCR was achieved using the same primers as used in Q-RT-PCR.

Western blotting. Proteins were isolated from cell cultures using M-Per Lysis Buffer (Thermo-Fisher Scientific, Perbio Science), and concentrations were evaluated using the Protein Assay Kit from Bio-Rad. Proteins were reduced using β-mercaptoethanol and immediately subjected to electrophoresis through 15% SDS polyacrylamide gels. After electrophoresis, proteins were transferred to nitrocellulose filters and soaked for 4 h 30 min at room temperature in Starting Block Blocking Buffer (STB; Thermo-Fisher Scientific, Perbio Science). Next, filters were incubated overnight at 4°C in STB, and the rabbit polyclonal antibody α-Rho-6005 directed against RhoH. Filters were then washed and incubated for 1 h at room temperature with a donkey anti-rabbit secondary antibody conjugated with horseradish peroxidase (HRP). Filters were again washed, and HRP was visualized using the ECL Western Blotting System purchased from Amersham Biosciences, GE Healthcare Europe, GmbH. The protein loading of gels was evaluated by hybridization with a mouse antibody directed against tubulin that was purchased from Sigma-Aldrich Chimie. The RhoH and tubulin signals were quantitated using a CanoScan LiDE 35 apparatus (Canon USA, Inc.) combined with ImageQuaNT software. The α-Rho-6005 antibody was generated by immunizing rabbits with a peptide of the sequence QARRRNRRRLFSINEC that represents amino acids 173 to 188 of the human RhoH protein (Eurogentec). Donkey anti-rabbit or sheep anti-mouse secondary antibodies conjugated with HRP were purchased from Amersham Biosciences, GE Healthcare Europe, GmbH.

Transfection. EH and Mo cells were transfected by electroporation using 1 μg of pRSV-β and 16 μg of pCMV-RhoH mixed with either 8 μg of pATLuc or 8 μg of p11c-Wt. As controls for these experiments, parallel transfections were performed with the empty parental vector pCMV from which pCMV-RhoH was derived. JOK-1 cells were transfected in the same way as EH and Mo, except that pCMV-RhoH was replaced with pMEP-RhoH and pCMV was replaced with pMEP4. In addition, the culture medium to which transfected JOK-1 cells were placed contained 1 μmol/L $CdCl_2$ to drive *RhoH* expression from the *metallothionine* promoter present in pMEP4. Evaluation of *RhoH* promoter activity was achieved by transfecting EH and Raji cells with 0.5 μg of pSV-βGal mixed with 4.5 μg of either pGL4-RhoH or pGL4.14[*Luc2/Hygro*].

Generation of stable cell line pools. The plasmids pMEP4 and pMEP-RhoH were linearized by digestion with *Cla*I and then transfected by electroporation into JOK-1 cells. Pools of JOK-1 cells that contained the transfected plasmids stably integrated within their genome were selected by treatment with 150 μg/mL of hygromycin.

Flow cytometric analysis. Flow cytometry of JOK-1 cells stably expressing *pMEP4* or *pMEP-RhoH* and cultured *in vitro* was performed by incubating 5×10^5 cells with a PE-conjugated version of the monoclonal antibody BU15 directed against CD11c (Beckman-Coulter). The isotype-matched control for these experiments used a PE-conjugated version of the IgG1 clone 679-Mc7 (Beckman-Coulter). After staining, cells were fixed with 1% paraformaldehyde and analyzed using an EPICS XL-MCL flow cytometer (Beckman-Coulter). Phenotypic evaluation of B-lymphocytes isolated from the peripheral blood of normal volunteers and HCL patients was performed by fluorescence-activated cell sorting analysis after double-labeling with anti–human-CD19 and anti–human-CD103 antibodies conjugated, respectively, with PE and FITC (Beckman-Coulter). Evaluation of mouse splenocytes and B-lymphocytes isolated from the spleens of patients with SLVL or ITP was performed using only the anti–human-CD19 antibody and its control.

Homotypic adhesion assays. Petri dishes were seeded with 5×10^5 cells/mL and incubated for 3 d. Representative fields of the cultures were photographed after 1 and 3 d using an inverted phase contrast microscope (DMIL, Leica) equipped with a video camera and Leica Q-fluoro Standard Image software. In parallel, the number and size of the aggregates in the cultures were evaluated using a Leica 52 7001 ocular objective equipped

Downloaded from cancerres.aacrjournals.org on January 5, 2016. © 2008 American Association for Cancer Research.

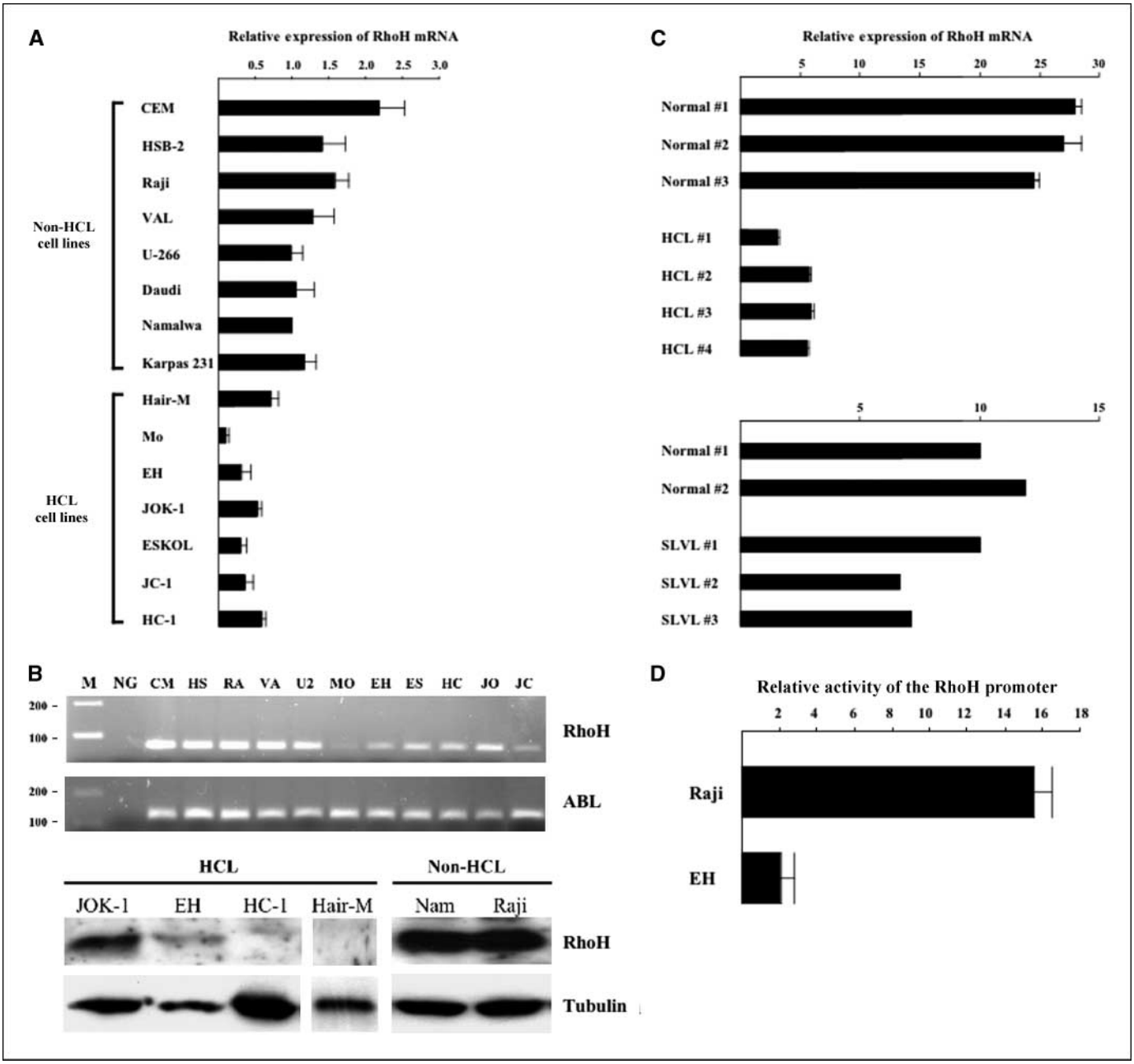

Figure 1. RhoH is underexpressed in HCL mediated by a transcriptional mechanism. *A,* total RNA was extracted from the HCL cell lines Hair-M, Mo, EH, JOK-1, ESKOL, JC-1, and HC-1. Total RNA was also extracted from the cell lines CEM and HSB-2 representing T-acute lymphoblastic leukemia, the cell lines Raji, Daudi, and Namalwa representing Burkitt's lymphoma, U-266 representing plasmocytoma, VAL representing B-cell non–Hodgkin's lymphoma, and Karpas 231 representing *de novo* acute leukemia of mature B-cells. The quantitative levels of RhoH and ABL expression were determined for each individual cell line by Q-RT-PCR. The relative level of endogenous RhoH expression was then calculated by dividing the quantitative level of RhoH expression by the quantitative level of ABL expression (45). *Columns,* mean of two independent experiments; *bars,* SE. *B, top,* agarose gel stained with ethidium bromide showing the products of RT-PCR reactions that evaluate the levels of RhoH and ABL mRNA expression in cell lines CEM (*CM*), HSB-2 (*HS*), Raji (*RA*), VAL (*VA*), U-266 (*U2*), Mo (*MO*), EH, ESKOL (*ES*), HC-1 (*HC*), JOK-1 (*JO*), and JC-1 (*JC*). *NG,* contains a PCR reaction performed with no cDNA template; *M,* contains DNA size markers. The size of these markers in base pairs is indicated on the left side of the figure. *Bottom,* total protein was extracted from the HCL B-cell lines JOK-1, EH, HC-1, and Hair-M and from the non-HCL B-cell lines Raji and Namalwa. 50 μg of EH protein, 100 μg of Namalwa, Raji, JOK-1, and Hair-M protein, and 150 μg of HC-1 protein were subject to SDS-PAGE followed by Western blotting. RhoH protein expression was analyzed using the rabbit polyclonal anti-RhoH antibody α-Rho-6005. Protein loading was checked by hybridizing the blots with an antitubulin antibody. Representative of two independent experiments. *C, top,* total RNA was extracted from the circulating B-lymphocytes of three normal individuals and from four patients with HCL. The relative levels of RhoH expression were then determined by Q-RT-PCR in the same way as for hematopoietic cell lines. *Columns,* mean of two independent experiments; *bars,* SE. *Bottom,* B-lymphocytes were isolated from the normal spleens of two patients with ITP and the pathologic spleens of three patients with SLVL. The relative levels of expression of RhoH mRNA were determined as in the top. *D,* a fragment of the *RhoH* gene representing nucleotides −236 to +67 relative to a transcription initiation site used in B-lymphocytes was cloned upstream of the *luciferase* gene in pGL4.14[*Luc2/Hygro*] to generate the construct pGL4-RhoH. The transfection control plasmid pSV-βGal was mixed with either the parental vector pGL4.14[*Luc2/Hygro*] or pGL4-RhoH. The two plasmid mixtures were then transfected into the HCL B-lymphocyte cell line EH or the non-HCL B-lymphocyte cell line Raji. The levels of β-galactosidase activity directed by pSV-βGal were taken as reflective of transfection efficiency and used to correct the luciferase assay results. After correction for transfection efficiency, the level of *luciferase* reporter gene activity directed by pGL4-RhoH above that conferred by pGL4.14[*Luc2/Hygro*] was calculated. *Columns,* mean of three independent experiments; *bars,* SE.

Downloaded from cancerres.aacrjournals.org on January 5, 2016. © 2008 American Association for Cancer Research.

with a micrometric grid of 1 mm^2 divided into 100 squares of 0.01 mm^2. All measurements represented the average values obtained from six representative fields of 1 mm^2. The size of the aggregates was evaluated as a function of time by measurement of their surface area expressed in mm^2. Aggregates were classified into the three size categories of small (0.1–0.25 × 0.01 mm^2), medium (0.5–1.0 × 0.01 mm^2), and large (1.5–20.0 × 0.01 mm^2). The percentage of aggregates in each category was then calculated using the formula: (number of clumps in a given category / total number of clumps) × 100. The percentage of cells that were not engaged in aggregates was also analyzed. In this case, measurements were averaged from 10 representative fields of 1 mm^2 and obtained by counting every cell not engaged in an aggregate. In parallel, 5 mL of the culture were removed; aggregates in this aliquot were disrupted by repeat pipetting, and the total number of cells was averaged from 10 representative fields of 1 mm^2. The percentage of nonaggregated cells was then calculated by dividing the average number of nonaggregated cells per 1 mm^2 field by the average total number of cells per 1 mm^2 field and multiplying this value by 100.

Lymphocyte-endothelial adhesion assays. Monolayers of the endothelial cell line HMEC-1 were seeded into 96-multiwell culture plates at a density that a previous experiment using crystal violet staining had shown produces confluency after 48 h. The resulting confluent monolayers were either left untreated or activated for 18 h with 100 ng/mL of LPS. Pools of JOK-1 cells stably transfected with pMEP4 or pMEP-RhoH were incubated for 30 min at 37°C in the presence of 5 μmol/L BCECF-AM (Calbiochem, EMD Biosciences, Inc.) then washed thrice in HBSS. Labeled cells (10^5) were added to each well containing activated or nonactivated monolayers, culture plates were then centrifuged for 4 min at 150 × *g* to affect uniform settling, and adhesion was allowed for 1 h at 37°C. Monolayers were then gently washed thrice in HBSS, and fluorescence intensity was measured at 485 nm using a Mithras LB 940 multimode reader (Berthold Technologies, GmbH & Co KG). All values were normalized by subtraction of the fluorescence intensity of monolayers incubated in buffer alone. Specific cell adhesion was assessed by subtracting the fluorescence intensities obtained from nonactivated monolayers from the intensities obtained using activated monolayers. Adhesion assays for each stable JOK-1 pool were performed a total of thrice at minimum in quadruplicate.

Transendothelial migration assays. Confluent monolayers of HMEC-1 were prepared in the same way as for leukocyte-endothelial adhesion assays but in Transwell migration chambers of 6.5-mm diameter and 5.0-μm pore size (Corning, Inc.). Transwell inserts were set in HMEC-1 medium carried in 24-well plates and either left untreated or activated for 18 h with 100 ng/mL of LPS. Next, 10^5 JOK-1 cells either stably expressing *pMEP4* or *pMEP-RhoH* were prepared in 150 μL of HMEC-1 medium without LPS and added to the monolayers inside the Transwell inserts. These inserts were again set into 24-well plates and incubated for 8 h. After this time, the HMEC-1 medium under the Transwell inserts was supplemented with 100 ng/mL LPS to act as a chemoattractant. The Transwell inserts were then incubated at 37°C for 16 h, and the JOK-1 cells that migrated through to the medium on their underside were collected and counted. Migration assays were performed in triplicate, a total of thrice for each stable JOK-1 pool cultured with either activated or quiescent HMEC-1.

Xenograft mouse model. Male SCID mice (CB17 PRKDC, Charles River Laboratories), age 7 wk, were injected i.p. with 10^7 JOK-1 cells suspended in RPMI 1640 without FBS. The JOK-1 cells that were injected either stably expressed *pMEP-RhoH* or the empty vector *pMEP4*. Control mice were injected with the RPMI 1640 vehicle alone. During the next 4 wk, the health of the mice was monitored, and if death occurred, analysis was performed immediately. After four weeks, surviving animals were sacrificed and their peritoneal cavity opened for tumor analysis. When present, tumors were dissected, their size measured, and photographs were taken. Two tumors were analyzed by cytometry to confirm they consisted of JOK-1 cells expressing human CD19. Spleens were also removed from injected mice, photographed, and weighed. This organ was then dilacerated, and its cellular contents were collected by irrigation with PBS. Erythrocytes present in the collection were lysed, and the remaining cells were subjected to cytometry analysis using an antibody that specifically recognizes human CD19 or an isotype-matched control antibody.

Results

RhoH is specifically underexpressed in cell lines derived from HCL. Previous studies have shown that the Ras family of proto-oncogenes is abnormally active in HCL (13, 25). Because RhoH represents a natural inhibitor of Ras in the hematopoietic lineage, we investigated the possibility that HCL may be characterized by RhoH underexpression. Initially, to address this question, we used Q-RT-PCR to examine RhoH mRNA levels in a

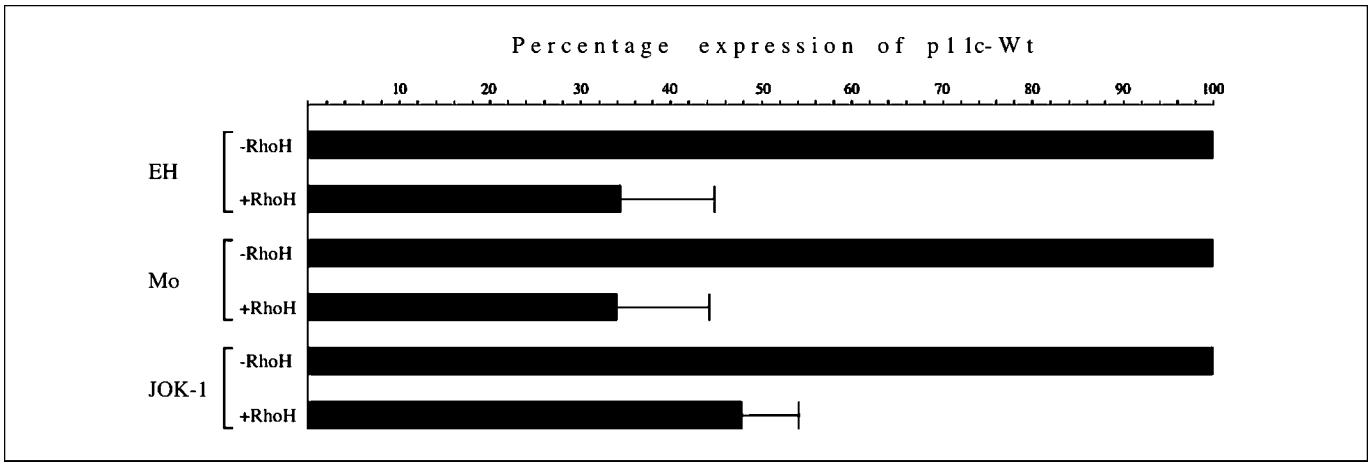

Figure 2. RhoH reconstitution in HCL represses *CD11c* promoter activity. A fragment of the *CD11c* gene representing nucleotides -128 to +36 relative to the major transcription initiation site was cloned upstream of the *luciferase* gene in pATLuc to generate p11c-Wt (13, 43, 44). EH, Mo, and JOK-1 cells were transfected in parallel with p11c-Wt and pATLuc, each mixed with the plasmid pRSV-β that constitutively expresses β-galactosidase. Transfections of EH and Mo were performed in the presence of pCMV-RhoH that constitutively expresses RhoH or in the presence of its empty equivalent pCMV. Transfections of JOK-1 were performed in the presence of pMEP-RhoH, where *RhoH* is expressed from the *metallothionine* promoter or the empty parental plasmid pMEP4. Transfected JOK-1 cells were cultured with 1 μmol/L $CdCl_2$, and transfected EH and Mo were cultured without $CdCl_2$ for 16 h before β-galactosidase and luciferase assays were performed. The levels of β-galactosidase activity were taken as reflective of transfection efficiency and used to correct the firefly luciferase assay results. After correction for transfection efficiency, the level of *luciferase* reporter gene activity directed by p11c-Wt above that conferred by pATLuc in the presence of pCMV or pMEP4 was assigned a value of 100% (−*RhoH*). The level of activity directed by p11c-Wt in parallel transfections in the presence of pCMV-RhoH or pMEP-RhoH is expressed as a percentage of this value (+*RhoH*). *Columns,* mean of three independent experiments; *bars,* SD.

Downloaded from cancerres.aacrjournals.org on January 5, 2016. © 2008 American Association for Cancer Research.

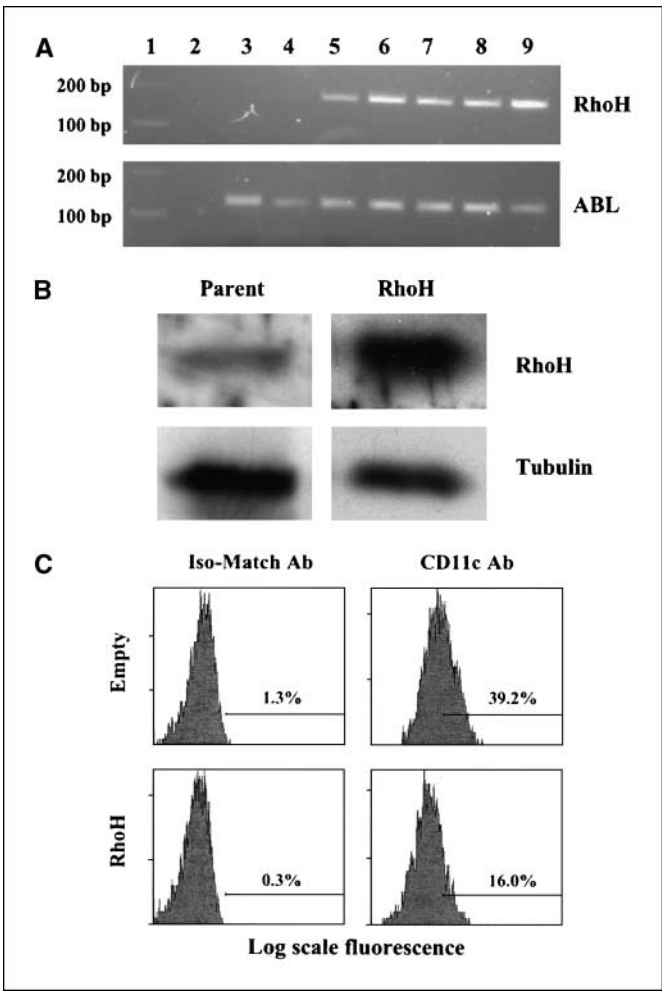

Figure 3. RhoH reconstitution reduces surface expression of CD11c. Pools of JOK-1 cells were generated that contain within their genome either *pMEP4* or *pMEP-RhoH*. *A,* agarose gel stained with ethidium bromide after electrophoresis of RT-PCR products generated from JOK-1 cells expressing *pMEP4* or *pMEP-RhoH*. The pairs of oligonucleotides used in the PCR generated products from mRNA encoding recombinant RhoH tagged with the VSVG epitope (*RhoH*) or from the *ABL* gene product (*ABL*). The oligonucleotides fail to generate products from endogenous RhoH mRNA. *Lane 1,* size markers; *lane 2,* RT-PCR product using distilled water as template; *lane 3,* RT-PCR product using as template mRNA isolated from JOK-1 carrying *pMEP4* and cultured in the absence of supplementary $CdCl_2$; *lane 4,* JOK-1 carrying *pMEP4* and cultured in the presence of 10 μmol/L supplementary $CdCl_2$; *lane 5,* JOK-1 carrying *pMEP-RhoH* and cultured in the absence of supplementary $CdCl_2$; *lane 6,* JOK-1 carrying *pMEP-RhoH* and cultured for 24 h with 1 μmol/L supplementary $CdCl_2$; *lane 7,* JOK-1 carrying *pMEP-RhoH* and cultured for 48 h with 1 μmol/L supplementary $CdCl_2$; *lane 8,* JOK-1 carrying *pMEP-RhoH* and cultured for 24 h with 10 μmol/L supplementary $CdCl_2$; *lane 9,* JOK-1 carrying *pMEP-RhoH* and cultured for 48 h with 10 μmol/L supplementary $CdCl_2$. This analysis showed that cells carrying *pMEP4* expressed no recombinant RhoH whereas cells carrying *pMEP-RhoH* produced recombinant RhoH either in the presence or absence of supplementary $CdCl_2$. *B,* Western blots of total protein extracted from parental JOK-1 cells (*Parent*) or JOK-1 stably expressing *pMEP-RhoH* (*RhoH*). Both cell lines were cultured in the absence of supplementary $CdCl_2$. Expression of RhoH was analyzed using the antibody α-Rho-6005 and protein loading analyzed with an antibody that recognizes tubulin. Representative of two independent experiments. *C*, flow cytometric analysis was performed on JOK-1 stably expressing *pMEP4* (*Empty*) and on JOK-1 cells stably expressing *pMEP-RhoH* (*RhoH*). Both cell lines were cultured in the absence of supplementary $CdCl_2$, and cytometry was performed using a monoclonal antibody that specifically binds CD11c (*CD11c Ab*) or an isotype matched control (*Iso-Match Ab*). The percentages of cells that exhibit fluorescence in a defined range of intensity are presented from a representative of three independent experiments. The mean reduction in CD11c expression determined from these experiments was 49.5% ±SD of 9%.

range of cell lines derived from both patients with HCL and other forms of leukemia. This study indicated that, on average, the relative expression of RhoH mRNA in HCL cell lines was 3.4-fold lower than that in cell lines derived from Burkitt's lymphoma (Raji, Daudi, and Namalwa), plasmocytoma (U-266), T-acute lymphoblastic leukemia (HSB-2 and CEM), *de novo* acute B-cell leukemia (Karpas 231), and B-cell non–Hodgkin's lymphoma (VAL; Fig. 1*A* and *B, top*). In addition to mRNA levels, RhoH protein levels were also significantly repressed in HCL cell lines compared with non-HCL cells (Fig. 1*B, bottom*). Specifically, we found RhoH protein to be undetectable in the HCL cell lines HC-1 and Hair-M and reduced 2.7-fold and 3.3-fold in EH and JOK-1, respectively, compared with its average expression in the Burkitt's lymphoma lines Raji and Namalwa.

RhoH is underexpressed in neoplastic lymphocytes isolated directly from HCL patients. Because RhoH seems underexpressed in HCL cell lines, we next wanted to determine whether this represented an accurate reflection of the malignant cells circulating within the blood stream of HCL patients. Therefore, we isolated B-lymphocytes from the blood of three normal donors and from four patients with HCL. Examination by Q-RT-PCR showed that RhoH expression levels were, on average, 5.2-fold lower in the B-lymphocytes of HCL patients compared with normal individuals (Fig. 1*C, top*). In contrast to this substantial suppression of RhoH in HCL lymphocytes, splenic B-lymphocytes isolated from patients with SLVL exhibited, on average, only a 27% reduction in RhoH expression (Fig. 1*C, bottom*).

RhoH underexpression in HCL cells is mediated by transcriptional repression of the *RhoH* gene promoter. RhoH underexpression in HCL could be mediated by transcriptional and/or posttranscriptional events. We investigated the former possibility by isolating the human *RhoH* promoter spanning nucleotides −236 to +67 relative to a transcription initiation site used in B-lymphocytes (46). This promoter region was then cloned upstream of the *luciferase* reporter gene present in pGL4.14[*Luc2/Hygro*] to generate the construct pGL4-RhoH. When pGL4-RhoH was transfected into EH hairy cells, it directed expression only 2.1-fold above that directed by pGL4.14[*Luc2/Hygro*] empty of *RhoH* gene sequences (Fig. 1*D*). In contrast, when pGL4-RhoH was transfected into the non–hairy cell B-lymphocyte cell line Raji, it directed expression 15.6-fold above background (Fig. 1*D*). Thus, the transcriptional activity of the wild-type *RhoH* promoter is 7.4-fold lower in HCL cells than in nonhairy cells. These results indicate that transcriptional repression of the *RhoH* gene promoter plays a major role in RhoH underexpression in HCL cells.

Transient reconstitution of RhoH expression represses the aberrant activity of the *CD11c* gene promoter that characterizes HCL. The β2-integrin CD11c is normally largely restricted in its expression pattern to cells of the myeloid lineage (11). Its abnormal expression on the surface of HCL lymphocytes is used as a diagnostic marker for the disease (9). In previous studies, we have shown that in HCL abnormal expression of the CD11c protein reflects abnormal transcription of the gene by which it is encoded (13). We have further shown that this abnormal transcription is Ras-dependent and driven by the promoter region of the *CD11c* gene extending from −128 to +36 relative to the major site of transcription initiation. Because high levels of Ras-dependent transcription from the *CD11c* promoter are characteristic of HCL, we sought to determine whether this might result from underexpression of RhoH. To test this possibility, we used the HCL cell lines Mo, EH, and JOK-1. A construct constitutively expressing

Downloaded from cancerres.aacrjournals.org on January 5, 2016. © 2008 American Association for Cancer Research.

human RhoH was transfected into these cell lines in combination with either a *CD11c* promoter construct or its parental vector empty of *CD11c* sequences. In Mo, EH, and JOK-1, the expression of exogenous RhoH caused, on average, 66%, 66%, and 52% reductions, respectively, in the transcriptional activity of the *CD11c* promoter (Fig. 2). These results showed that RhoH repression contributes to the expression of the *CD11c* promoter in hairy cells.

Stable reconstitution of RhoH expression reduces cell surface expression of CD11c protein. In JOK-1 hairy cells, transient reconstitution of RhoH expression represses the *CD11c* gene promoter when the promoter is present in an extrachromosomal plasmid (Fig. 2). Next, we investigated the possibility that RhoH reconstitution might also cause a reduction in the surface expression of the CD11c protein, as this would reflect repression of the endogenous *CD11c* gene. Pools of JOK-1 that contain genomic integration of either an empty expression plasmid or this same plasmid constitutively expressing RhoH were generated (Fig. 3*A* and *B*). The surface expression of CD11c in these two pools of cells was then assessed using flow cytometry. This analysis established that stable reconstitution of RhoH expression causes, on average, a 49.5% decrease in CD11c expression (Fig. 3*C*). Consequently, in JOK-1 cells, reconstitution inhibits endogenous, as well as exogenous, *CD11c* expression.

Reconstitution of RhoH expression inhibits the homotypic adhesion of HCL. One of the hallmarks of HCL is the extravasation of neoplastic lymphocytes (1–3). Such extravasation is dependent upon malignant cells exhibiting increased intercellular adhesion. In cell culture, this increased capacity for adhesion is manifest by HCL cell lines typically growing in large clumps. We have shown that RhoH reconstitution in HCL reduces expression of the proadhesion molecule CD11c. Others have shown that RhoH holds the CD11a/CD18 heterodimer in an inactive conformation (47). Because RhoH seems to inhibit functional expression of molecules that mediate leukocyte adhesion, we tested the hypothesis that RhoH reconstitution in HCL might inhibit homotypic intercellular adhesion. The pools of JOK-1 that either stably express RhoH or an empty vector were disrupted into cultures of single cells and then incubated undisturbed for 3 days (Fig. 4*A*). After this period of time, we found that, compared with the pools expressing the empty vector, the pools expressing RhoH had over 5-fold fewer cells growing as aggregates (Fig. 4*B*). In

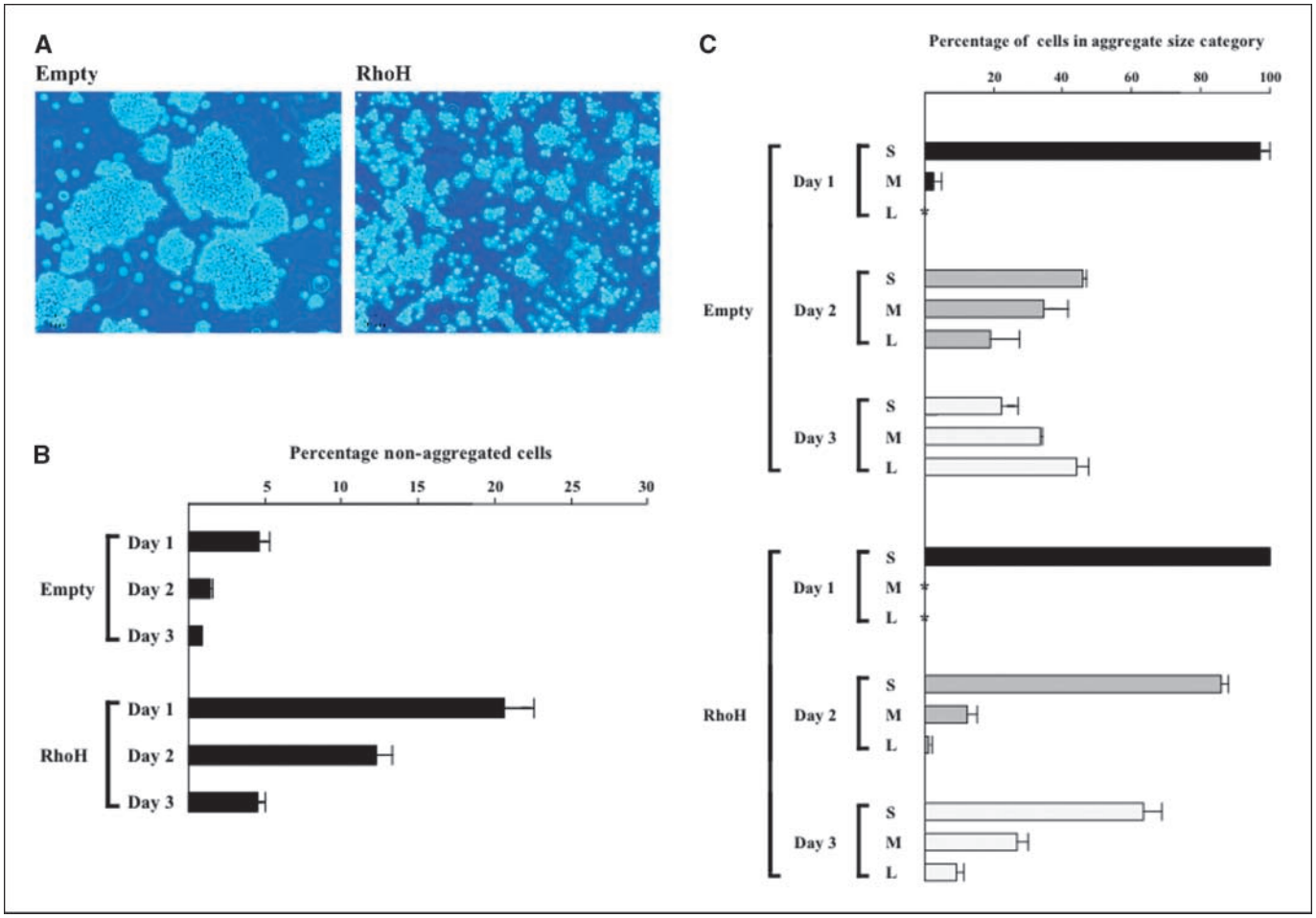

Figure 4. Reconstitution of RhoH expression in HCL inhibits homotypic adhesion. *A,* light microscope images of JOK-1 cells that contain in their genome either *pMEP4* (*Empty*) or *pMEP-RhoH* (*RhoH*). Cells were photographed 3 d after a culture of single cells was initiated in the absence of supplementary $CdCl_2$. *B,* the percentage of cells not present in an aggregate of two or more. These values were calculated each day for 3 d after single-cell cultures were initiated from 0.5×10^6 JOK-1 cells that stably express either *pMEP4* or *pMEP-RhoH*. *Columns,* mean of 10 microscopic fields of 1 mm^2 of two independent experiments; *bars,* SE. *C,* the percentage of cells present in aggregates classified as small (*S*; 0.1–0.25 × 0.01 mm^2), medium (*M*; 0.5–1.0 × 0.01 mm^2), or large (*L*; 1.5–20.0 × 0.01 mm^2). These values were calculated each day for 3 d after single-cell cultures were initiated. *Columns,* mean of six microscope fields of 1 mm^2 of two independent experiments; *bars,* SE. Asterisks denote values of 0%.

Downloaded from cancerres.aacrjournals.org on January 5, 2016. © 2008 American Association for Cancer Research.

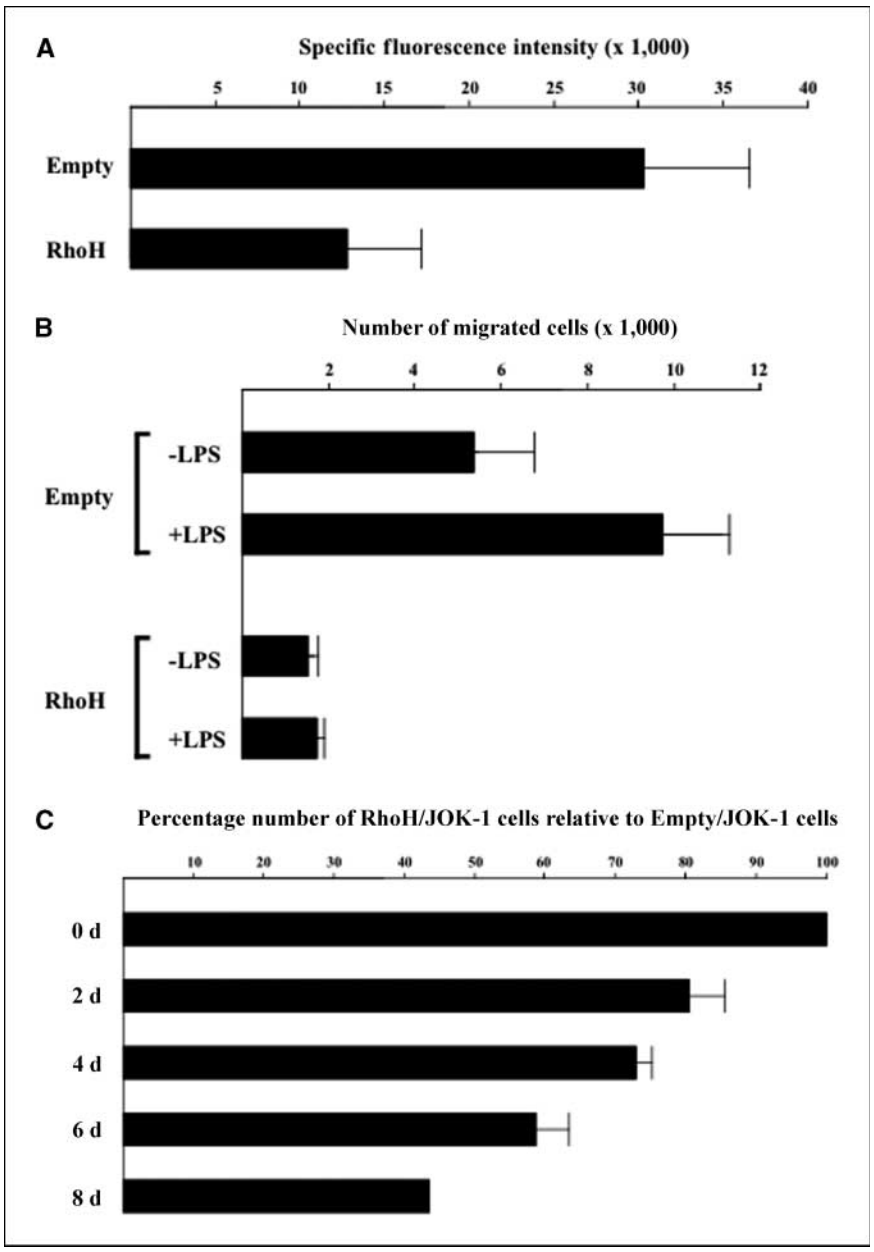

Figure 5. Reconstitution of RhoH inhibits heterotypic adhesion, transendothelial migration, and proliferation. *A,* pools of JOK-1 cells stably transfected with pMEP4 (*Empty*) or pMEP-RhoH (*RhoH*) were cultured in the absence of supplementary $CdCl_2$ and labeled with the fluorescent marker BCECF. Cells were then incubated for 1 h with monolayers of HMEC-1 activated or untreated with LPS. Monolayers were then gently washed, and fluorescence intensity was measured at 485 nm. All values were normalized by subtraction of the fluorescence intensity of monolayers incubated in buffer alone. Specific fluorescence intensity was then determined by subtracting the fluorescence intensity obtained from nonactivated monolayers from that obtained using monolayers activated with LPS. *Columns,* mean of three independent experiments; *bars,* SD. *B,* JOK-1 cells stably transfected with pMEP4 (*Empty*) or pMEP-RhoH (*RhoH*) were cultured in the absence of supplementary $CdCl_2$ and then settled on top of quiescent (−*LPS*) or activated (+*LPS*) monolayers of HMEC-1 within Transwell migration chambers. After 8 h, the culture medium present below the HMEC-1 monolayers was supplemented with 100 ng/mL LPS to act as a chemoattractant for the JOK-1 cells. At 16 h later, the JOK-1 cells that migrated through the support membrane of the endothelial monolayer were collected and counted. *Columns,* mean of three independent experiments; *bars,* SD. *C,* equal numbers of JOK-1 cells containing *pMEP4* or *pMEP-RhoH* were cultured in parallel, and after 0, 2, 4, 6, and 8 d, the cells were counted. The growth medium used in these experiments did not contain supplementary $CdCl_2$. The number of cells containing the empty vector *pMEP4* was assigned a value of 100%, and the number of cells containing *pMEP-RhoH* was calculated as a percentage of this value. *Columns,* mean of two independent experiments; *bars,* SE.

addition, the sizes of the aggregates that did exist were significantly reduced (Fig. 4*C*).

Reconstitution of RhoH expression inhibits the heterotypic adhesion of HCL. Our study of aggregation indicated that RhoH reconstitution in HCL cells inhibits their homotypic adhesion (Fig. 4). However, central to the process of HCL extravasation is the heterotypic adhesion of malignant cells to vascular endothelium. The ability of RhoH reconstitution to inhibit this kind of adhesion was assessed *in vitro* using a fluorescence assay we have previously used (48). Use of this assay showed that the pools of JOK-1 hairy cells reconstituted with RhoH exhibit a 58% reduction in adhesion to activated endothelial cells compared with control pools (Fig. 5*A*).

Reconstitution of RhoH expression inhibits HCL transendothelial migration. In addition to simple endothelial adhesion, HCL extravasation is dependent upon malignant cells being able to migrate through endothelium. Consequently, using Transwell migration chambers, we assessed the ability of RhoH reconstitution to inhibit HCL transendothelial migration. Equal numbers of control JOK-1 pools and pools reconstituted with RhoH were settled for 8 hours on top of quiescent or activated endothelial monolayers. JOK-1 migration was then elicited by adding LPS to the culture medium present below the monolayers. After 16 hours, the JOK-1 cells that had migrated both through the endothelial monolayer, as well as its support membrane, were collected and counted. With quiescent endothelial monolayers, JOK-1 cells reconstituted with RhoH exhibited a 3.5-fold reduction in migration capacity compared with control cells. When endothelial monolayers were activated, the degree of reduction reached 5.5-fold (Fig. 5*B*). This more pronounced reduction was caused by endothelial activation inducing the migration of control cells by 81% but inducing the migration of cells reconstituted with RhoH by only 16%.

Reconstitution of RhoH expression reduces HCL proliferation. Abnormal intercellular adhesion that effects transendothelial

Downloaded from cancerres.aacrjournals.org on January 5, 2016. © 2008 American Association for Cancer Research.

migration represents one of the pathologic hallmarks of HCL. The finding that such processes are dependent upon underexpression of RhoH suggests that reconstitution of RhoH may represent a useful therapeutic strategy. We further assessed this possibility by determining the ability of RhoH reconstitution to block HCL proliferation. Cultures were initiated from equal numbers of the JOK-1 pools that contained stable integration of an empty vector or this same vector expressing RhoH. The two pools were cultured in parallel, and after 0, 2, 4, 6, and 8 days, the cells were counted. The number of cells containing the empty vector was assigned a value of 100%, and the number of cells containing the RhoH plasmid was calculated as a percentage of this value. The results depicted in

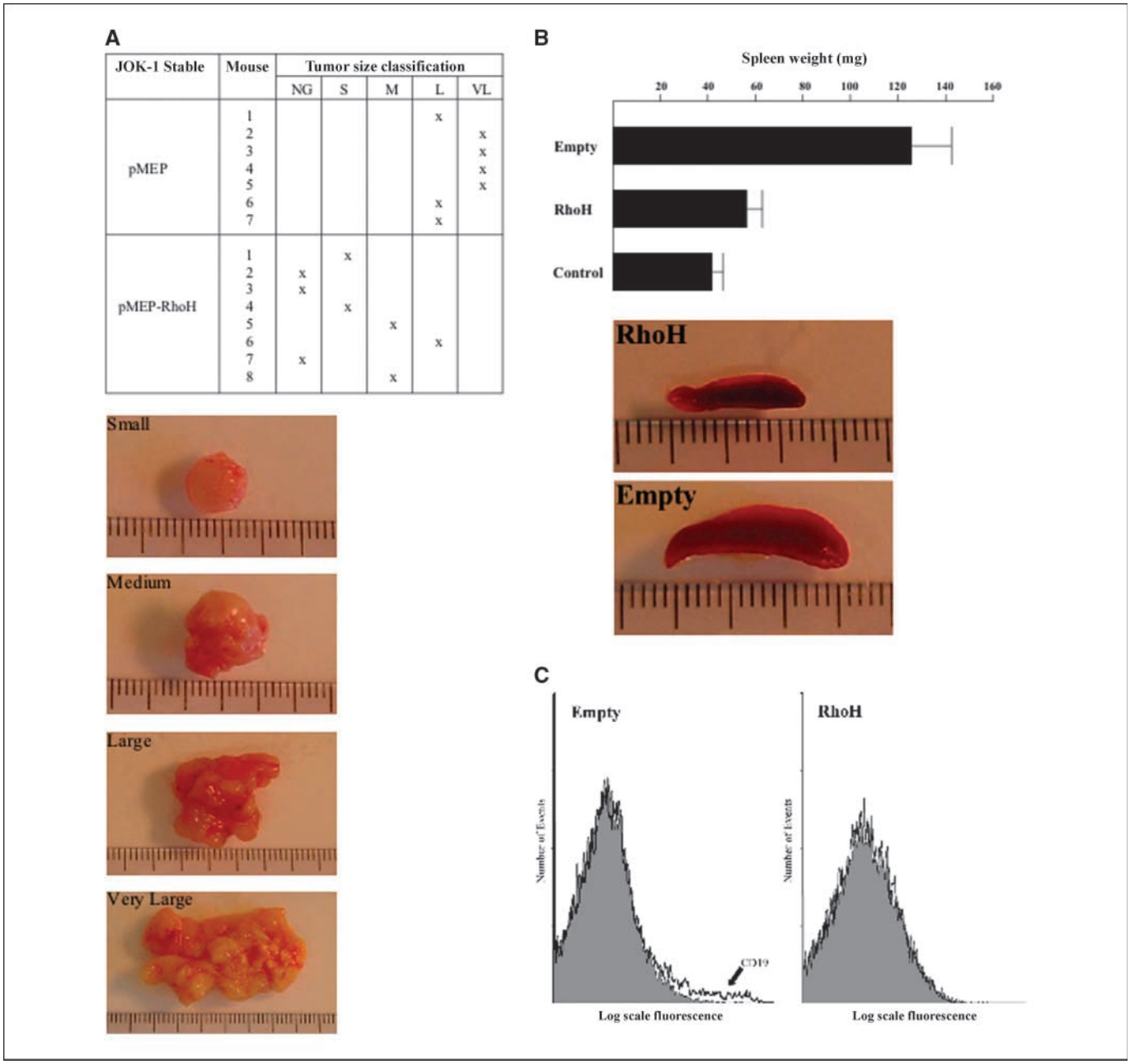

JOK-1 Stable	Mouse	Tumor size classification				
		NG	S	M	L	VL
pMEP	1				x	
	2					x
	3					x
	4					x
	5					x
	6				x	
	7				x	
pMEP-RhoH	1		x			
	2	x				
	3	x				
	4		x			
	5			x		
	6				x	
	7	x				
	8			x		

Figure 6. RhoH reconstitution inhibits malignant progression *in vivo*. The peritoneum of SCID mice was injected with RPMI1640, RPMI1640 containing JOK-1 cells stably expressing the empty vector *pMEP4*, or RPMI1640 containing JOK-1 cells stably expressing the RhoH expression construct *pMEP-RhoH*. After 28 d, all surviving mice were sacrificed and the injection site and/or spleens were examined. *A, top,* seven mice that received cells expressing *pMEP4* and eight mice that received cells expressing *pMEP-RhoH* were classified depending upon whether they had no visible tumor (*NG*), a small tumor of <1 cm in maximum diameter (*S*), a medium sized tumor of 1 to 1.4 cm (*M*), a large tumor of 1.5 to 2.4 cm (*L*), or a very large tumor of 2.5 to 3.5 cm (*VL*). *Bottom,* photographs of representatives of each tumor class. The smallest division of the ruler depicted in each image is 1 mm. *B, top,* weight of the spleens isolated from mice injected with RPMI 1640 alone (*Control*) or mice injected with JOK-1 cells expressing either *pMEP4* (*Empty*) or *pMEP-RhoH* (*RhoH*). *Columns,* mean weight of 4, 9, and 12 mice, respectively; *bars,* SE. *Bottom,* representatives of spleens isolated from mice injected with JOK-1 cells expressing either *pMEP4* (*Empty*) or *pMEP-RhoH* (*RhoH*). The smallest division of the ruler depicted in each image is 1 mm. *C,* a representative of cytometric analysis of human CD19 expression in spleen B-lymphocytes isolated from nine mice injected with JOK-1 cells expressing *pMEP4* (*Empty*) or 12 mice expressing *pMEP-RhoH* (*RhoH*). Reactivity with the antihuman CD19 antibody that detects injected JOK-1 cells is indicated by the open line. This line is overlaid with a filled line indicating reactivity with an isotype-matched negative control antibody.

Downloaded from cancerres.aacrjournals.org on January 5, 2016. © 2008 American Association for Cancer Research.

Fig. 5*C* indicate that RhoH reconstitution causes a reduction in HCL proliferation, such that after 8 days, the number of JOK-1 cells was reduced, on average, by 57%.

RhoH reconstitution protects against malignant progression *in vivo*. Our data generated *in vitro* show that RhoH reconstitution inhibits both the proliferation and adhesion of HCL cells. Next, we used a xenograft mouse model to determine whether RhoH reconstitution inhibits malignant progression *in vivo*. The JOK-1 pools that contained stable integration of an empty vector or this same vector expressing RhoH were injected into the peritoneum of SCID mice. Twelve mice were injected with each pool. During the course of 28 days, all mice injected with cells reconstituted with RhoH remained alive and vigorous. In contrast, all mice injected with nonreconstituted cells became increasingly sluggish with three dying at day 27. After 28 days, all surviving animals, including the vigorous subjects injected with RhoH reconstituted cells were sacrificed. The peritoneal cavity was opened, and the site of injection was examined in seven recipients of nonreconstituted cells and eight recipients of reconstituted cells. In the eight examined recipients of HCL cells reconstituted with RhoH, three failed to develop any manifestation of malignancy, two developed tumors of <1 cm in maximum dimension, and the other three had tumors of maximum dimension of 1.2, 1.4, and 1.8 cm. These observations were in striking contrast to mice injected with HCL cells not reconstituted with RhoH expression. Here, the seven mice examined all developed tumors of at least 2.1 cm maximum dimension, and two had tumors of a maximum dimension over 3 cm (Fig. 6*A*). Taken together, these data generated using mice indicate that reconstituting RhoH expression reduced HCL tumor burden by 70%. Further analysis indicated that RhoH reconstitution eliminated splenomegaly (Fig. 6*B*). In addition, the percentage of JOK-1 cells present in the spleen was reduced from 1.6% to 0% (Fig. 6*C*).

Discussion

We report here that HCL lymphocytes exhibit constitutive underexpression of RhoH mediated by repression of its gene promoter. Reconstitution of RhoH expression *in vitro* inhibits HCL proliferation, adhesion, and transendothelial migration. Use of a xenograft mouse model indicates that RhoH reconstitution limits malignant progression *in vivo*.

Cell proliferation is driven by Ras activation (49). Because RhoH is a negative regulator of the Ras family, this provides a molecular explanation for RhoH reconstitution being able to inhibit HCL proliferation. The ability of RhoH reconstitution to inhibit the transendothelial migration that results from HCL exhibiting increased intercellular adhesion can be explained in two ways. First, RhoH has been shown to hold the adhesion receptor CD11a/CD18 in an inactive form (47). Second, RhoH reconstitution is able to inhibit transcription of the gene that encodes the leukocyte adhesion molecule CD11c (Fig. 2). This inhibition is likely effected by inhibiting ras-signaling cascades. Such cascades we have shown to be abnormally activated in HCL leading to constitutive expression of the transcription factor AP-1 and subsequent induction of *CD11c* gene transcription.

Disclosure of Potential Conflicts of Interest

No potential conflicts of interest were disclosed.

Acknowledgments

Received 9/27/2007; revised 3/5/2008; accepted 3/31/2008.

Grant support: Institut de Recherches sur le Cancer de Lille, Comité du Nord of Ligue Nationale Française Contre le Cancer, Region Nord Pas-de-Calais, Institut National de la Santé et de la Recherche Médicale, and Hairy Cell Leukemia Research Foundation.

The costs of publication of this article were defrayed in part by the payment of page charges. This article must therefore be hereby marked *advertisement* in accordance with 18 U.S.C. Section 1734 solely to indicate this fact.

We thank Guy Faguet, Edward Sour, Jorn Koch, and Sean Colgan for providing the cell lines; Christophe Roumier for providing the normal blood samples; Nathalie Jouy for help with flow cytometry analyses; Harold Fauvel for help with fluorometry; Maud Collyn d'Hooghe, Anne-Sophie Harzfeld, Hélène Leroy, and Paul Peixoto for help with photography and assays of adhesion and migration; Institut National de la Santé et de la Recherche Medicale IFR114, IMPRT, and EPER in Lille for use of their Beckman Coulter cytometry apparatus, their Applied Biosystems ABI-Prism 7700 quantitative PCR apparatus, and their Mithras Berthold fluorometry apparatus; and Claude Denis and Isabelle Briche for excellent technical assistance.

References

1. Bouroncle BA, Wiseman BK, Doan CA. Leukemic reticuloendotheliosis. Blood 1958;13:609–30.
2. Allsup DJ, Cawley JC. Diagnosis, biology and treatment of hairy-cell leukaemia. Clin Exp Med 2004;4:132–8.
3. Platanias LC, Golomb HM. Hairy cell leukaemia. Baillieres Clin Haematol 1993;6:887–98.
4. Robak T. Current treatment options in hairy cell leukemia and hairy cell leukemia variant. Cancer Treat Rev 2006;32:365–76.
5. Mey U, Strehl J, Gorschluter M, et al. Advances in the treatment of hairy-cell leukaemia. Lancet Oncol 2003;4:86–94.
6. Zypchen LN, Nantel SH, Barnett J, Noble M, Gascoyne RD, Connors JM. Cladribine does not cure hairy cell leukemia (HCL) [ASH abstract 1593]. Blood 2003.
7. Golde DW, Stevens RH, Quan SG, Saxon A. Immunoglobulin synthesis in hairy cell leukemia. Br J Haematol 1977;35:359–65.
8. Saxon A, Stevens RH, Golde DW. T-lymphocyte varient of hairy-cell leukemia. Ann Int Med 1978;88:323–6.
9. Schwarting R, Stein H, Wang CY. The monoclonal antibodies αS-HCL1 (αLeu-14) and αS-HCL3 (αLeu-M5) allow the diagnosis of hairy cell leukemia. Blood 1985;65:974–83.
10. Yam LT, Li CY, Lam KW. Tartrate-resistant acid phosphatase isoenzyme in the reticulum cells of leukemic reticuloendotheliosis. N Engl J Med 1971;284:357–60.
11. Arnaout MA. Structure and function of the leukocyte adhesion molecules CD11/CD18. Blood 1990;75:1037–50.
12. Lam KW, Li O, Li CY, Yam LT. Biochemical properties of human prostatic acid phosphatase. Clin Chem 1973;19:483–7.
13. Nicolaou F, Teodoridis JM, Park H, et al. *CD11c* gene expression in hairy-cell leukemia is dependent upon activation of the proto-oncogenes *ras* and *junD*. Blood 2003;101:4033–41.
14. Shaulian E, Karin M. AP-1 in cell proliferation and survival. Oncogene 2001;20:2390–400.
15. Abate C, Patel L, Rauscher FJ III, Curran T. Redox regulation of fos and jun DNA-binding activity *in vitro*. Science 1990;249:1157–61.
16. Boyle WJ, Smeal T, Defize LHK, et al. Activation of protein kinase C decreases phosphorylation of c-jun at sites that negatively regulate its DNA-binding activity. Cell 1991;64:573–84.
17. Angel P, Imagawa M, Chiu R, et al. Phorbol ester-inducible genes contain a common cis element recognized by a TPA-modulated transacting factor. Cell 1987;49:729–39.
18. Lamph WW, Wamsley P, Sassone-Corsi P, Verma IM. Induction of proto-oncogene JUN/Ap-1 by serum and TPA. Nature 1988;334:629–31.
19. Angel P, Hattori K, Smeal T, Karin M. The jun proto-oncogene is positively autoregulated by its product, Jun/Ap-1. Cell 1988;55:875–85.
20. Wilson T, Treisman R. Removal of poly(A) and consequent degradation of c-fos mRNA facilitated by 3′ AU-rich sequences. Nature 1988;336:396–9.
21. Nakamura T, Datta R, Kharbanda S, Kufe D. Regulation of jun and fos gene expression in human monocytes by the macrophage colony-stimulating factor. Cell Growth Differ 1991;2:267–72.
22. Abate C, Luk D, Curran T. A ubiquitous nuclear protein stimulates the DNA-binding activity of fos and jun indirectly. Cell Growth Differ 1990;1:455–62.
23. Abate C, Luk D, Gentz R, Rauscher FJ III, Curran T. Expression and purification of the leucine zipper and DNA-binding domains of Fos and Jun: both Fos and Jun contact DNA directly. Proc Natl Acad Sci U S A 1990;87:1032–6.
24. Xanthoudakis S, Curran T. Identification and characterization of Ref-1, a nuclear protein that facilitates AP-1 DNA-binding activity. EMBO J 1992;11:653–65.
25. Harvey WH, Harb OS, Kosak ST, Sheaffer JC, Lowe LR, Heerema NA. Interferon-α-2b downregulation of oncogenes H-ras, c-raf-2, c-kit, c-myc, c-myb and c-fos in ESKOL, a hairy cell leukemic line, results in temporal perturbation of signal transduction cascade. Leuk Res 1994;18:577–85.
26. Dallery E, Galiègue-Zouitina S, Collyn-d'Hooghe M, et al. TTF, a gene encoding a novel small G protein, fuses to the lymphoma-associated LAZ3 gene by t(3, 4) chromosomal translocation. Oncogene 1995;10:2171–8.

Downloaded from cancerres.aacrjournals.org on January 5, 2016. © 2008 American Association for Cancer Research.

27. Dallery-Prudhomme E, Roumier C, Denis C, Preudhomme C, Kerckaert JP, Galiègue-Zouitina S. Genomic structure and assignment of the RhoH/TTF small GTPase gene (ARHH) to 4p13 by *in situ* hybridization. Genomics 1997;1:89–94.

28. Li X, Bu X, Lu B, Avraham H, Flavell RA, Lim B. The hematopoietic-specific GTP-binding protein RhoH is GTPase deficient and modulates activities of other Rho GTPases by an inhibitory function. Mol Cell Biol 2002;22: 1158–71.

29. Gu Y, Jasti AC, Jansen M, Siefring JE. RhoH, a hematopoietic-specific Rho GTPase, regulates proliferation, survival, migration, and engraftment of hematopoietic progenitor cells. Blood 2005;105:1467–75.

30. Kalyanaraman VS, Sarngadharan MG, Robert-Guroff M, Miyoshi I, Golde D, Gallo RC. A new subtype of human T-cell leukemia virus (HTLV-II) associated with a T-cell variant of hairy cell leukemia. Science 1982;218:571–3.

31. Foley GE, Lazarus H, Farber S, Uzman BG, Boone BA, McCarthy RE. Continuous culture of human lymphoblasts from peripheral blood of a child with acute leukemia. Cancer 1965;18:522–9.

32. Adams RA, Flowers A, Davis BJ. Direct implantation and serial transplantation of human acute lymphoblastic leukemia in hamsters, SB-2. Cancer Res 1968;28: 1121–5.

33. Nadkarni JS, Nadkarni JJ, Clifford P, Manolov G, Fenyo EM, Klein E. Characteristics of new cell lines derived from Burkitt lymphomas. Cancer 1969;23:64–79.

34. Pulvertaft JV. Cytology of Burkitt's tumor (African lymphoma). Lancet 1964;39:238–40.

35. Nilsson K, Bennich H, Johansson SG, Ponten J. Established immunoglobulin producing myeloma (IgE) and lymphoblastoid (IgG) cell lines from an IgE myeloma patient. Clin Exp Immunol 1970;7:477–89.

36. Kerckaert JP, Deweindt C, Tilly H, Quief S, Lecocq G, Bastard C. LAZ3, a novel zinc-finger encoding gene, is disrupted by recurring chromosome 3q27 translocations in human lymphomas. Nat Genet 1993;5:66–70.

37. Nacheva E, Dyer MJ, Fischer P, et al. C-MYC translocations in *de novo* B-cell lineage acute leukemias with t(14; 18; cell lines Karpas 231 and 353). Blood 1993; 82:231–40.

38. Schiller JH, Bittner G, Meisner LF, et al. Establishment and characterization of an Epstein-Barr virus spontaneously transformed lymphocytic cell line derived from a hairy cell leukemia patient. Leukemia 1991; 5:399–407.

39. Faguet GB, Satya-Prakash KL, Agee JF. Cytochemical, cytogenetic, immunophenotypic and tumorigenic characterization of two hairy cell lines. Blood 1988;71:422–9.

40. Harvey W, Srour EF, Turner R, et al. Characterization of a new cell line (ESKOL) resembling hairy-cell leukemia: a model for oncogene regulation and late B-cell differentiation. Leuk Res 1991;15:733–44.

41. Kontula K, Paavonen T, Vuopio P, Andersson LC. Glucocorticoid receptors in hairy-cell leukemia. Int J Cancer 1982;30:423–6.

42. Ades EW, Candal FJ, Swerlick RA, et al. HMEC-1: establishment of an immortalized human microvascular endothelial cell line. J Invest Dermatol 1992;99: 683–90.

43. Shelley CS, Farokhzad OC, Arnaout MA. Identification of cell-specific and developmentally regulated nuclear factors that direct myeloid and lymphoid expression of the CD11a gene. Proc Natl Acad Sci U S A 1993;90:5364–8.

44. Shelley CS, Teodoridis JM, Park H, Farokhzad OC, Böttinger EP, Arnaout MA. During Differentiation of the monocytic cell line U937, Purα mediates induction of the *CD11c* gene promoter. J Immunol 2002;168:3887–93.

45. Gabert J, Beillard E, van der Velden VH, et al. Standardization and quality control studies of "real-time" quantitative reverse transcriptase polymerase chain reaction of fusion gene transcripts for residual disease detection in leukemia-a Europe Against Cancer program. Leukemia 2003;17:2318–57.

46. Lahousse S, Smorowski AL, Denis C, Lantoine D, Kerckaert JP, Galiègue-Zouitina S. Structural features of hematopoiesis-specific RhoH/ARHH gene: high diversity of 5′-UTR in different hematopoietic lineages suggests a complex post-transcriptional regulation. Gene 2004;343: 55–68.

47. Cherry LK, Li X, Schwab P, Lim B, Klickstein LB. RhoH is required to maintain the integrin LFA-1 in a nonadhesive state on lymphocytes. Nat Immunol 2004;5: 961–7.

48. Kong T, Eltzschig HK, Karhausen J, Colgan SP, Shelley CS. Leukocyte adhesion during hypoxia is mediated by HIF-1 dependent induction of β2 integrin gene expression. Proc Natl Acad Sci U S A 2004;101:10440–5.

49. Giehl K. Oncogenic Ras in tumour progression and metastasis. Biol Chem 2005;386:193–205.

Downloaded from cancerres.aacrjournals.org on January 5, 2016. © 2008 American Association for Cancer Research.